THE INTERNATIONAL JOURNAL OF MEDICAL ROBOTICS AND COMPUTER ASSISTED SURGERY
Int J Med Robotics Comput Assist Surg 2006; **2**: 75–83.
Published online in Wiley InterScience (www.interscience.wiley.com). **DOI:** 10.1002/rcs.82

ORIGINAL ARTICLE

Integrated image- and function-guided surgery in eloquent cortex: a technique report†

James P. O'Shea
Stephen Whalen
Daniel M. Branco
Nicole M. Petrovich
Kyle E. Knierim
Alexandra J. Golby*

Brigham and Women's Hospital and Harvard Medical School, Boston, MA 02115, USA

*Correspondence to:
Alexandra J. Golby, Department of Neurosurgery, Brigham and Women's Hospital, 75 Francis Street, Boston, MA 02115, USA.
E-mail: agolby@bwh.harvard.edu

†No conflict of interest was declared.

Accepted: 25 January 2006

Abstract

The ability to effectively identify eloquent cortex in close proximity to brain tumours is a critical component of surgical planning prior to resection. The use of electrocortical stimulation testing (ECS) during awake neurosurgical procedures remains the gold standard for mapping functional areas, yet the preoperative use of non-invasive brain imaging techniques such as fMRI are gaining popularity as supplemental surgical planning tools. In addition, the intraoperative three-dimensional display of fMRI findings co-registered to structural imaging data maximizes the utility of the preoperative mapping for the surgeon. Advances in these techniques have the potential to limit the size and duration of craniotomies as well as the strain placed on the patient, but more research accurately demonstrating their efficacy is required. In this paper, we demonstrate the integration of preoperative fMRI within a neuronavigation system to aid in surgical planning, as well as the integration of these fMRI data with intraoperative ECS mapping results into a three-dimensional dataset for the purpose of cross-validation. Copyright © 2006 John Wiley & Sons, Ltd.

Keywords functional MRI; electrocortical stimulation testing; brain tumour; brain mapping; neuronavigation

Introduction

Maximal surgical excision is currently the best treatment option for brain tumours since complete excision can extend survival, decrease mass effect, lessen the risk of progression to higher grade, reduce the incidence of seizures, and render patients eligible for adjuvant therapies (1). Achieving this desired outcome is often problematic, however, given that the optimal limits of resection are not always clear. This is particularly true when tumours are within or adjacent to eloquent cortex, and may variably infiltrate, distort or displace functional tissue. In these situations, the surgeon is faced with the difficult decision of how far to carry the surgical resection, knowing that the risk of permanent neurological deficit must be weighed against the goal of complete resection.

Performing brain surgery with the patient awake under local anaesthesia allows monitoring of the neurological integrity of the patient, and the use of electrocortical stimulation testing (ECS) to investigate function at the time of surgery (mimicking a temporary surgical lesion) remains the current gold standard for defining the safe limits of resection. The application of this technique, in conjunction with the widespread adoption of intraoperative neuronavigation, has given surgeons significantly more intraoperative information for surgical decision-making. Since this method depends on preoperative imaging data, however, its accuracy may be compromised as

a result of the brain shift which can occur once the dura is opened (2,3). Intraoperative MRI, which helps the surgeon to distinguish between tumour and adjacent brain, can provide updated imaging data to compensate for some of the error associated with this brain shift (4). Such facilities, however, are extremely resource-intensive and thus available in only a limited number of centres. Moreover, the operative constraints within the intraoperative-MRI environment (instrumentation, electrocorticography, positioning, etc.) mean that, for many cases, it may not be the best environment.

Preoperative functional mapping has the potential to help delineate the relationship between tumour and healthy tissue, and enhance the utility of the imaging data used for surgical planning. As a non-invasive technique for functional mapping, it provides an alternative method for determining critical brain regions without subjecting the patient to additional strain. Its application is particularly useful given that some studies have identified the presence of functional brain tissue within some glial tumours (5). Finally, as minimally invasive techniques are developed to treat brain lesions (e.g. focused ultrasound), non-invasive brain mapping techniques will be required to guide the deployment of these techniques in individual patients (6).

Functional MRI

Since its early development, there has been tremendous enthusiasm for the potential of fMRI as a clinical tool, especially with regard to functional mapping for brain surgery. FMRI is non-invasive, has an excellent signal : noise ratio (SNR), and is able to demonstrate task-associated brain activity in single subjects. The physiological basis of fMRI depends on neuronally mediated vasodilation that occurs in response to localized neuronal activation. This results in an increase in the ratio of oxyhaemoglobin to deoxyhaemoglobin and can be imaged on T2*-weighted images as the blood oxygen level-dependent (BOLD) signal. However, there is little understanding about how pathological processes (e.g. tumours) may affect neurovascular coupling. Additionally, in order for fMRI and other non-invasive brain mapping techniques to be useful for clinical neurosurgical planning, they must be validated against the gold standard of intraoperative ECS.

Past research has demonstrated some fairly gross validation of basic motor and language function using fMRI and ECS, and several recent studies have shown more quantitative comparisons between these methods. Hirsch *et al*. (7) made qualitative assessments of correlation based upon visual inspection of intraoperative photographs. Using landmark-based methods, Yetkin *et al*. (8) and Roux *et al*. (9) co-registered digitized photos to functional data before calculating the ECS and fMRI spatial agreement. In several more recent studies, Krings *et al*. (10), Roux *et al*., (11) and Pirotte *et al*. (12) have directly measured the distances between integrated ECS and fMRI data within the neuronavigation systems after registering the preoperative fMRI data to the patient position. The tolerance for registration errors in these studies was in the range 3–5 mm, when reported.

Despite this progress, questions regarding the usefulness of fMRI surgical planning and the accuracy of these methods remain. In part, this is due to the relatively gross spatial resolution of standard fMRI studies, resulting in functional activation that is not sufficiently finely localized within the cortex for surgical planning. A second significant obstacle is determining an effective false-positive rate at which to threshold the fMRI activation data. Given the individual differences in BOLD signal intensity and statistical significance levels, many studies have applied a range of thresholds to each subject, rather than choosing a single fixed value (7,10–13). A further difficulty with the use of preoperative imaging data for intraoperative navigation, as stated before, is the instance of volumetric brain deformation that can result from the craniotomy. At our institution we have developed a protocol for the intraoperative display of preoperatively acquired fMRI data, for the digitization of cortical stimulation sites and responses, and for the postoperative integration of these data for correlation analyses. This technique may be important to combine the advantages of both fMRI and ECS for surgical decision making, to evaluate the differences between these two methods and to validate fMRI. Post-operative reconstruction of the datasets, including the position of the cortex during three-dimensional (3D) mapping, can also allow for some determination of brain shift.

Patients and methods

Patients were recruited from the multi-disciplinary brain tumour clinic at Brigham and Women's Hospital. Between February 2003 and March 2005, 10 patients with brain tumours and/or epileptogenic foci within or adjacent to the primary somatosensory-motor area or probable language areas, and who were candidates for awake surgery with motor or language mapping, were prospectively enrolled. Patients gave informed consent in accordance with the Partner's Healthcare IRB protocols. See Table 1 for patient information.

Pre-surgical fMRI acquisition

Functional MRI was performed using a 3 Tesla scanner at Brigham and Women's Hospital. A T2-weighted image and a high-resolution T1-weighted gradient echo 3D image were acquired for anatomical co-registration. Whole-brain functional sequences were acquired with a T2*-weighted echo-planar sequence sensitive to the blood oxygen-level dependent signal (TR, 2000 ms; TE, 30 ms; matrix, 64 × 64 mm; FOV, 240 mm; imaging 24 contiguous slices of 5 mm thickness). Stimuli were presented using a PC laptop (Dell Inc., Austin, TX) running E-prime (Psychology

Table 1. Summary of patient clinical findings

Patient	Study	Gender	Age	Brain pathology	Operative location	Intraoperative tasks	Intraoperative notes
1	Lesion	M	40	Anaplastic glioma	Right temporoparietal	Motor mapping	Positive mapping; biopsy only
2	Lesion	M	34	Glioblastoma	Right frontotemporal	Motor mapping	Negative mapping; consistent with fMRI
3	Lesion	M	57	Glioma	Left temporal	Object-naming, number-counting	Positive mapping; consistent with fMRI
4	Lesion	F	46	Mixed oligoastrocytoma	Right frontal	Motor mapping	Positive mapping; biopsy only
5	Lesion	F	48	Glioblastoma	Left frontal	Motor mapping	Negative mapping; SMA
6	Epilepsy/lesion	M	41	Vascular cavernous malformation	Left frontal	Object-naming, number-counting	Positive mapping; consistent with fMRI
7	Lesion	M	27	Mass; residual infiltrating glioma	Left temporal	Object-naming, number-counting	Positive mapping
8	Epilepsy	F	35	Fragments of cerebral cortex with reactive changes	Anterior left temporal	NA	Extra-operative mapping
9	Epilepsy	M	39	Cerebral cortex and subcortical white matter with focal destructive changes	Left anterior temporal lobectomy and amygdalo-hippocampectomy	Object-naming	Intra- and extra-operative mapping
10	Lesion	F	51	Anaplastic astrocytoma	Left frontal	Number-counting	Positive mapping

Software Tools, Pittsburgh, PA) and presented to the patient on an MR-compatible goggle system (Resonance Technology Inc., Northridge, CA) that was also used for intraoperative presentation of stimuli.

Functional MRI behavioural paradigms

Patients performed a clinically relevant subset of tasks from a battery of motor and language paradigms. Motor tasks consisted of both active and passive finger-tapping and hand-clenching. Passive tasks were implemented using a custom-built MR-compatible pneumatically-driven finger-moving device (14). Language tasks included verb generation, visual sentence comprehension [SCOLP: speed and capacity of language processing test (15)], and object-naming. All tasks were implemented as block paradigms, alternating between task blocks and rest.

Functional MRI data analysis

Images were motion-corrected to the anatomical scans using SPM2 (Wellcome Department of Cognitive Neurology, London, UK), which uses a least-squares cost function and 4th degree B-spline interpolation method (16). Results from the motion-correction were rejected if the cumulative movement in any direction was beyond 3 mm. Co-registration of the functional data to the structural MRI was also conducted using SPM2, which implements an algorithm to maximize the mutual information of the joint probability distribution between the target volume and the source volume (17). The success of the co-registration was assessed based upon a visual inspection, and the results were rejected if the error appeared greater than 3 mm. Spatial smoothing was not performed in order to preserve the improved spatial resolution of the high-resolution echo planar functional images (18). Data were analysed using the general linear model (16). Differences between stimulus and baseline conditions (based upon the timing of stimulus presentation convolved with the haemodynamic response curve) were examined using analysis of co-variance with global signal and low frequency components treated as nuisance co-variates. Correction for multiple comparisons was performed using the theory of Gaussian random fields (19). The resulting maps of activated voxels were thresholded at false-positive rates individually chosen for each patient to qualitatively optimize the area of activation in the vicinity of the lesion. Because the threshold at which fMRI activation is displayed can significantly affect the extent of activation and thus its correspondence to the ECS sites, we additionally generated activation maps showing only the local maxima of the clusters. Tasks showing the most robust and consistent activation were selected for integration with the neuronavigation system during surgery. Figure 1 provides an example from one patient.

Integration of functional data with neuronavigation system

Neuronavigation during surgery was performed using an InstaTrak 3500 (GE Healthcare Navigation, Lawrence, MA) frameless stereotactic system, which allows up to five MR or CT volumes to be loaded simultaneously during a surgical procedure. A T1-weighted MPRAGE structural MRI scan was first loaded to serve as the primary reference for neuronavigation. Functional results from the fMRI data analyses were integrated into the neuronavigation system as the second volume by overlaying the activated voxels on a structural scan and converting the new volume to Digital Imaging and Communications in Medicine (DICOM) format, using the headers from the raw structural images (20). Our implementation of this method first required the intensity scale of the structural volume to be truncated at 99.95% of its maximum voxel intensity in order to make the upper range of

DOI: 10.1002/rcs

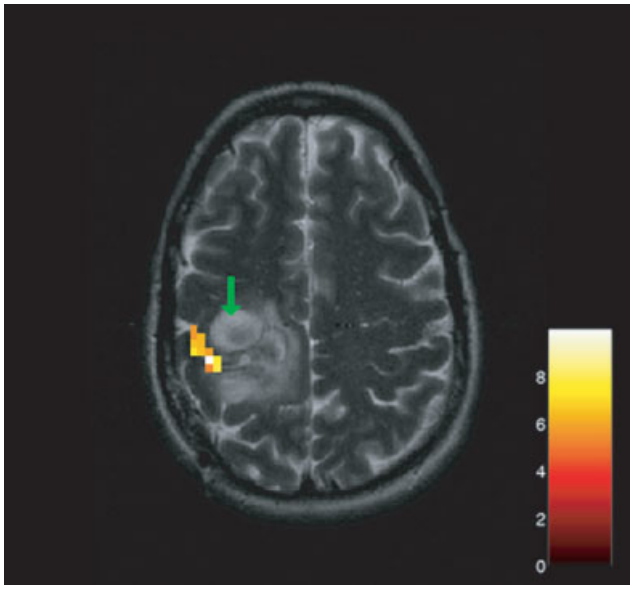

Figure 1. Preoperative fMRI activation from patient 4 for the left-hand active motor task, thresholded at $p < 0.05$ and corrected for multiple comparisons. The underlying T2-weighted structural image shows the right-frontal mixed oligoastrocytoma in the region of primary sensori-motor cortex (green arrow)

the gray-scale range (the very brightest) available for the functionally activated voxels. We then thresholded the activation maps of the functional data at the specified false-positive rate and increased by a constant offset the intensity values of the remaining voxels, such that the minimum activated voxel intensity was still greater than the maximum intensity of the truncated structural voxels. We then overlaid the modified voxels on the truncated structural image, putting them in the upper range of the intensity scale and effectively making them the brightest voxels in the new volume. The data from this combined volume were then appended to DICOM headers from the original structural scans. After loading this functional volume onto the neuronavigation system, we co-registered it to the reference volume using the InstaTrak's built-in automatic fusion algorithm, which is based on the maximization of mutual information (17).

The accuracy in the co-registration of functional data to the neuronavigation MRI volume was assessed using (a) a calculated error term, and (b) visual inspection of the resulting transformation. Errors were first assessed using manually placed landmarks to recalculate the transformation matrix. The surgeon visually checked the success of the co-registration by comparing structural landmarks between the functional data and the clinical navigation scan. The neuronavigation system also calculates an RMS error term, and the registration was typically rejected and performed again if the error was more than 2 mm. Upon successful co-registration, the volume containing the functional data was thresholded to the intensity level at which only the activated pixels remained. 3D models of the activation clusters were then generated using the neuronavigation system's built-in software, allowing direct intraoperative 3D comparisons with the electrocorticography and ECS sites (Figure 2).

Intraoperative procedure

All patients underwent awake craniotomy and intraoperative electrocortical mapping of eloquent cortex around the area of the proposed resection according to previously described techniques (21). Patient analgesia was maintained by local anaesthesia and limited intravenous sedation with short-acting agents. Surgical planning and navigation for ECS during mapping was conducted using the InstaTrak frameless stereotactic system. The patient position was co-registered to the neuronavigation MRI volume using a proprietary surface-based method which matches points on the patient's scalp to the reference MRI volume. As with the registration between this volume and the functional data, the system calculates an RMS error and the results were rejected if it exceeded approximately 2 mm.

Cortical mapping

The mapping procedure was initiated once the dura was opened and the effects of sedation diminished for the patient. To limit differences between preoperative and intraoperative mapping paradigms, patients were presented identical visual stimuli via the same display goggles employed during the fMRI session. Electrocortical stimulation testing was conducted using an Ojemann bipolar stimulator (inter-contact distance 5 mm) set to deliver a 75 Hz square wave with a pulse of 0.2 ms duration. During testing, the current was increased at each test site from 2 mA to 10 mA in 2 mA increments until the threshold for after-discharges was reached or a positive functional response was observed in the patient. Electrophysiological responses were monitored via intracranial EEG electrodes applied to the cortical surface. Prior to stimulation testing, the positions of the individual electrodes were registered on the neuronavigation system using the system's hand-held tracking probe, the accuracy of which is within 0.4 mm. As stimulation testing progressed, the position of each stimulation site was also registered on the neuronavigation system as a new point. For each stimulation test, we recorded the settings and position of the bipolar stimulator as well as any patient functional responses or electrophysiological events. Tissue resection was not performed within 1 cm of any positive ECS sites. These electrode and stimulation sites were displayed on the 3D model of the cortical surface alongside the functional data throughout the procedure (Figures 2, and 3). Any significant volumetric brain deformations which may have resulted from the craniotomy would also have been revealed by comparing the position of the electrode and stimulation sites to the cortical surface model generated from the preoperative data. If brain shift occurred, the sites would appear above or below the surface of the model (Figure 4).

DOI: 10.1002/rcs

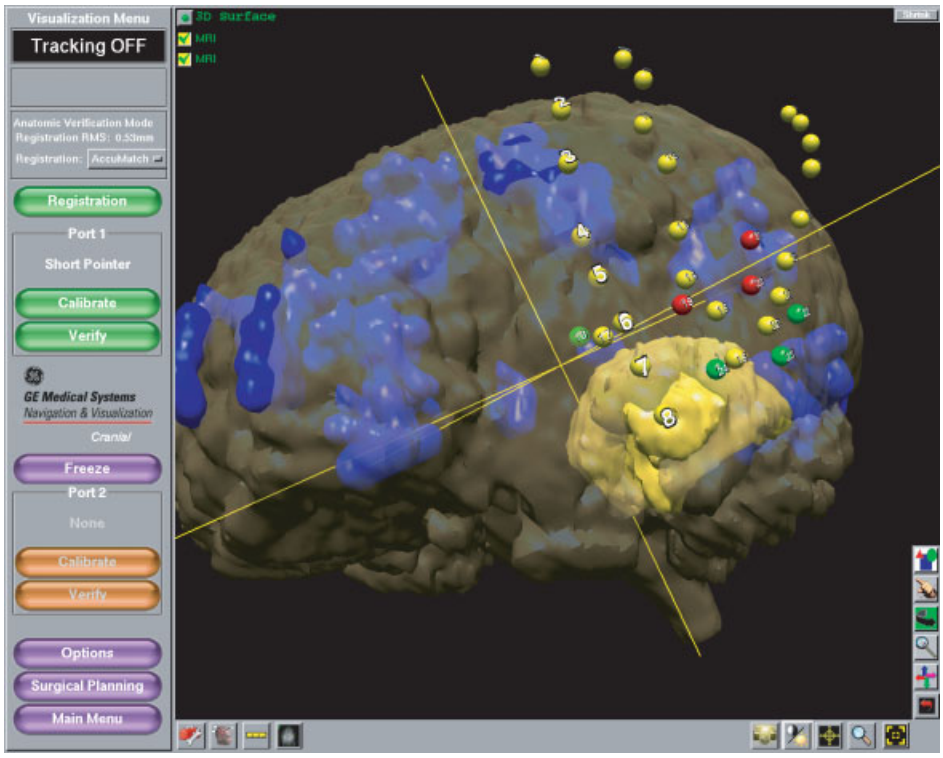

Figure 2. Intraoperative neuronavigation screenshot from patient 7, depicting the fMRI activation (blue) alongside the segmented left-temporal mass (yellow), electrode sites (yellow markers), negative ECS sites (green markers) and positive ECS sites (red markers). Due to the limited size of the craniotomy, some of the electrodes were placed under the dura beyond the reach of the hand-held neuronavigation probe. These positions were estimated on the scalp surface, and they appear several millimetres above the cortical model in the 3D display

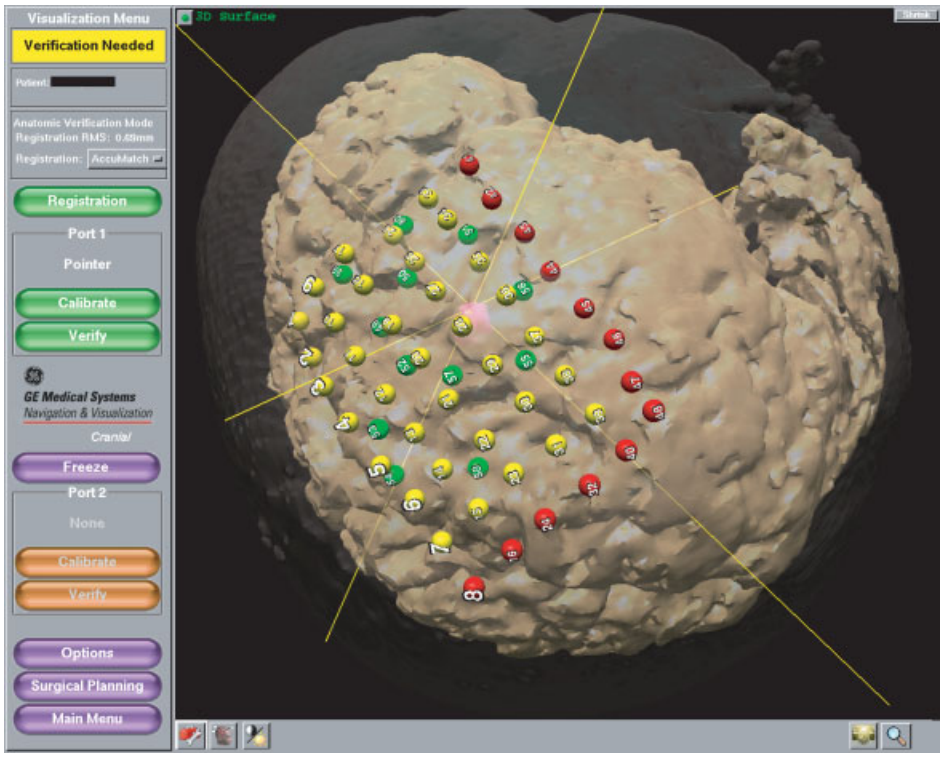

Figure 3. Intraoperative neuronavigation screenshot from patient 4. The lesion is the pink mass at the intersection of the cross-hairs. From the 48-electrode grid placed on the cortical surface for electrophysiological monitoring, 35 electrodes (yellow) maintained contact with the cortical surface. The remaining 13 electrodes (red) did not maintain sufficient contact for an adequate signal. Electrocortical stimulation sites are depicted in green (stimulation point tags are not colour-coded for patient response in this example)

DOI: 10.1002/rcs

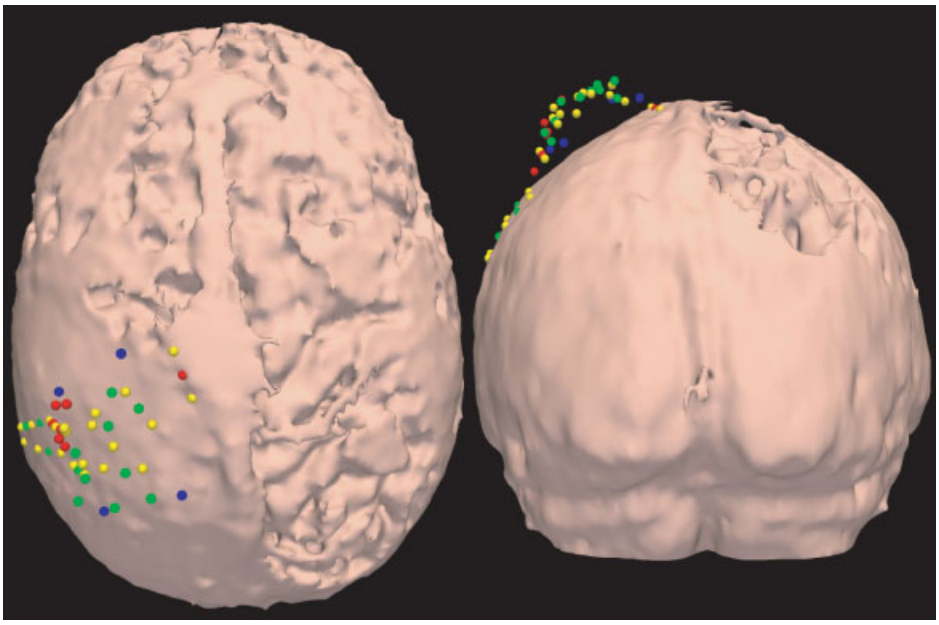

Figure 4. Superior and posterior views of a 3D rendering of a patient's cortical surface (preoperative data) overlaid with markers representing the positions of electrodes and stimulation sites from the surgical procedure (intraoperative data). The posterior view illustrates how these positions can effectively reveal the extent to which volumetric deformations of the brain occurred after the dura was opened. In this case, the actual intraoperative cortical surface within the craniotomy (delineated approximately by the blue markers) was displaced out of the skull as a result of the effect of gravity and the orientation of the head

Postoperative integration of fMRI and ECS data

Following intracranial functional mapping, the coordinates of the electrocorticography and ECS sites were saved in Extensible Markup Language (XML) format and transferred off-line to workstations outside the operating room for postoperative data analysis. The 3D Slicer software application (22) was used to integrate and visualize the preoperative MR volumes and functional data with the intraoperative ECS results and 3D models. Electrocorticography and ECS test sites were converted to the application's native file format and rendered as 3D model points alongside the models of the brain anatomy (Figure 5). Cross-validation of ECS and preoperative functional data was achieved using a custom software module, built into the 3D Slicer application, which calculated the Euclidean distance between specified sites and the edges of the 3D models representing the functional activity. In addition, the distances between specified sites and the local maxima of the fMRI activation clusters were similarly measured. These data are summarized in Table 2.

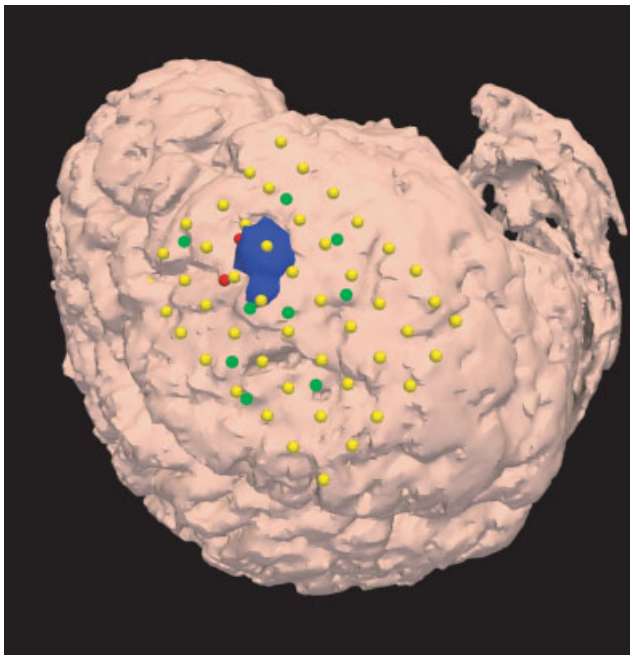

Figure 5. Offline view from the 3D Slicer application of the data for patient 4, including fMRI activation from the active left-hand motor task (blue). Positive ECS sites are depicted in red, negative ECS sites are green and electrodes are yellow. The tumour is not visible in this rendering because the cortical surface is opaque

Results

Patient outcome

All patients tolerated the preoperative fMRI studies and yielded interpretable results. In addition, all of the patients tolerated awake surgery and were able to cooperate with ECS testing. Two patients with epilepsy underwent medial temporal lobectomy. Of patients with lesions, two had biopsies of the lesion, five had gross total resection and one had a subtotal resection. One patient had transient word finding difficulty that resolved by discharge and one had transient reading difficulty that also resolved over 2 weeks. Two patients with left temporal lobe lesions had improved

DOI: 10.1002/rcs

Table 2. Summary of the distances (mm) between positive ECS sites and fMRI activation for successful intraoperative mapping cases. Distances were measured from both from the edge of fMRI clusters and the clusters' local maxima

		Cluster edge				Cluster max			
Patient	Sites (*n*)	Min	Max	SD	Mean	Min	Max	SD	Mean
1	0	NA	NA	NA	NA	NA	NA	NA	NA
2	2	0.8	3.6	2	2.2	15	15.2	0.2	15.1
3	5	3.7	18.6	6.3	8.5	15.4	39.2	9.1	26.2
4	3	21.8	27.7	3.1	25.3	26.9	36.2	5.4	33.1
5	1	8.7	8.7	NA	8.7	19.9	19.9	NA	19.9

speech postoperatively. There were no new permanent neurological deficits seen.

fMRI and ECS cross-validation

Results from the electrocortical stimulation testing were successfully collected for 7/10 patients. For the three cases that failed to yield useful intraoperative data, the patients underwent positive intraoperative mapping but ECS results were not recorded due to technical difficulties. Of the remaining seven cases, four resulted in positive intraoperative mapping results (a minimum of one stimulation site producing a functional response in the patient), enabling a direct comparison with the fMRI results. The other three cases did not yield positive stimulation sites, due either to the distant location of the resection site (consistent with fMRI results) or because extra-operative (rather than intraoperative) mapping was conducted in conjunction with epileptic monitoring.

A positive response to cortical stimulation depended on the location of the test site and the task being administered. For language tasks, positive responses included speech hesitation and arrest. For motor tasks, we included self-report of tingling or numbness as well as any overt movements or twitches. Due to the limited size of some craniotomies, it was not always possible to test locations in perfect correspondence to fMRI activation.

We calculated the euclidean distance between ECS sites and fMRI activation, using both the edge of the activation clusters as well as the cluster maxima to define the functional location (Table 2). Although the positive sites were generally closer to the fMRI activation than the negative sites, there were too few data points to warrant tests of statistical inference. In addition, the distribution of stimulation sites was not random, limiting our ability to lend significance to the patient responses. Using the entire fMRI activation clusters from the positive mapping cases, the mean distance to the edge of activation was 11.9 ± 3.0 mm for positive ECS sites compared to 16.8 ± 2.3 mm for negative sites. Figure 5 depicts the data from patient 4. When limiting the activation to only include the local maxima of the clusters adjacent to the area of the lesion, the mean distances to the positive and negative ECS sites were not significantly different (positive sites, 25.5 ± 2.7 mm; negative sites, 26.7 ± 2.1 mm), although the mean distance from the positive sites to the local maxima was less than the mean distance for negative sites for all four cases. Table 2 summarizes the distances from the ECS sites to the local maxima of the fMRI clusters. Figure 6 depicts these data from patient 4.

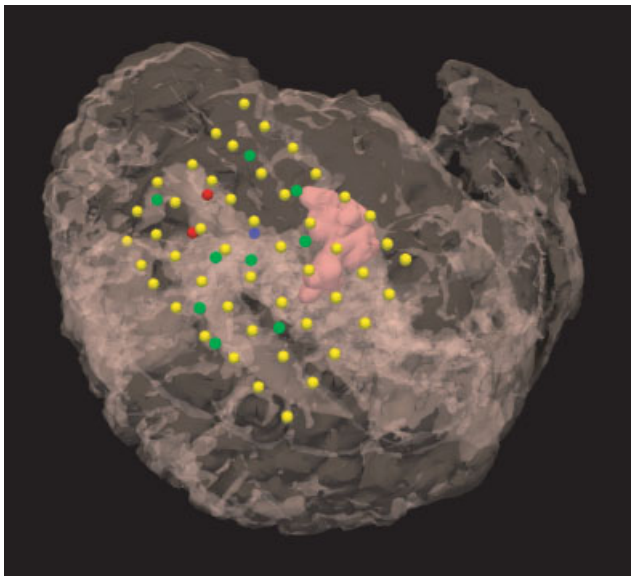

Figure 6. Offline view from the 3D Slicer application of the data for patient 4, with only the local maximum of the fMRI activation (blue) displayed from the active left-hand motor task. Because the local maximum was several millimetres below the cortical surface, the model of the cortical surface was rendered to be transparent, revealing the lesion (pink mass). The positive ECS sites are depicted in red, negative ECS sites in green and electrodes in yellow

Discussion

Identifying cortical areas essential for key brain functions is of critical importance in order to limit neurological deficits from lesion resection. The many advantages of preoperative imaging techniques do not yet outweigh the reliability of intraoperative ECS, and research validating the use of fMRI surgical mapping is ongoing. How best to perform, analyse, and present fMRI data will require continued study across institutions. Effectively confirming the usefulness of these techniques requires a dependable mechanism for integrating the functional data with the neuronavigation system, as well as the use of a software platform capable of correlating multi-modal data sets in a single 3D environment.

The present study demonstrates how fMRI data for preoperative functional mapping can be successfully integrated into a frameless stereotactic neuronavigation system to allow direct 3D comparison with intraoperative data. This implementation enhances the utility of preoperative mapping and provides a greater degree of assistance to the surgeon for surgical planning by allowing intraoperative visualization and reference to the patient's brain and the lesion. In addition, we describe

DOI: 10.1002/rcs

how ECS results can be intraoperatively recorded and further analysed postoperatively in an effort to validate the location of the fMRI activation and measure its effectiveness as a preoperative surgical planning tool.

Although recent studies have demonstrated direct quantitative comparisons of preoperative functional imaging data integrated with intraoperative neuronavigation data (11,12,23–26), most have only been implemented intraoperatively using the neuronavigation system. Our postoperative integration of the fMRI and ECS results within an experimental software platform (3D Slicer) enables a more thorough analysis of the data using a wider array of customized software modules. Besides the functionality to correlate the position of stimulation sites and the fMRI activation, the platform allows the integration of data from different modalities. Not only will this provide useful complementary information, but this effort will also allow the cross-validation of methods that depend on different physiologic signals. We acknowledge that it is not possible to demonstrate that these techniques improve clinical outcomes without a prospective randomized study.

Positive stimulation sites did not clearly correspond to fMRI activation in all cases. Discrepancies between functionally active areas identified via ECS and the clusters activated during fMRI can partly be explained by the intrinsic differences between the two modalities. Although fMRI may effectively identify areas of the brain active during certain tasks, these areas are not necessarily essential for task execution. The threshold at which fMRI activation is displayed can also significantly influence the degree to which stimulation sites correspond to functionally active areas. We avoid some of the ambiguity associated with choosing a threshold by correlating ECS site positions to the local maxima of the fMRI clusters in addition to the cluster edges.

The volumetric deformation of the brain which can occur during a craniotomy presents one of the more elusive problems complicating accurate intraoperative neuronavigation. Although previous studies have quantitatively verified the instance of cortical surface displacements during craniotomies (27), for most surgeries this brain shift is an unavoidable occurrence. The use of intraoperative MRI can help identify deformations by providing updated imaging data (28), but only a small subset of cases can usually be conducted in this environment, even at sites offering such a service. Given that a majority of neurosurgical cases are still conducted using image-guided methods based on preoperative imaging data, the best hope to account for brain shift is in the use of techniques such as finite element modelling, updated imaging, or sparse data collection (ultrasound, laser scanning). Our group is currently engaged in developing these types of multi-modal data integration techniques for validation in the intraoperative MRI system (29,30), yet many of these methods are still years from gaining widespread adoption for routine clinical use. While brain shift may contribute to inaccuracies in the fMRI/ECS comparisons based on neuronavigation systems using preoperative data, it still remains a much better method than the use of cortical landmarks. Moreover, error due to brain shift is minimal at the start of the case, during which time ECS testing is conducted. It has also been shown that displacements usually occur in the direction of gravity, which is primarily perpendicular to the surface of the cortex and therefore may have a limited effect on measuring fMRI/ECS correspondence (27).

The method by which distances between positive ECS sites and the fMRI activations were measured could also affect how closely the two mapping techniques coincide. A different correspondence might have been found if measurements were only calculated along the cortical surface instead of measuring the Euclidean distance in three-dimensional space, yet it is unclear which technique more effectively measures true concordance between the modalities. This uncertainty surrounding the correlation method highlights the importance of the 3D integration of data. Measuring the distances alone may not definitively resolve all the differences between ECS and fMRI, emphasizing the intraoperative utility of a complete 3D dataset for the surgeon to use for visual guidance.

Despite the numerous potential sources of error in using preoperative imaging data for intraoperative surgical planning, this technique is still useful and reasonably accurate, given the lack of demonstrably better alternatives. Although error can be introduced during the required co-registration steps, the total error is unlikely to exceed 1 cm, given the maximum tolerance for error permitted at each instance. It would be ideal to marginalize error completely, but even the use of ECS, the current gold-standard for intraoperative functional mapping, requires an allowance of up to 1 cm of error in defining the limits of resection. By quantitatively limiting the maximum error in each step of processing, we can effectively maintain a reasonable level of uncertainty when applying this technique.

Conclusion

A major challenge faced in brain tumour surgery is the identification and preservation of eloquent cortex in order to maintain the patient's neurological function. Functional MRI is a promising modality, allowing assessment of individual functional anatomy in relation to the tumour prior to surgery. In the present study, we have developed a technique for intraoperatively presenting fMRI data to the surgeon after integrating it into the neuronavigation platform. We are able to create 3D volumes which demonstrate fMRI activations in the context of the segmented tumour and brain surface. We are then able to superimpose the intraoperative cortical testing results by digitizing the stimulation points. This provides a 3D intraoperative structural and functional map that allows the surgeon to integrate and view all of the available information and use these to guide surgical decision making. In addition, we are able to accurately

DOI: 10.1002/rcs

measure direct correlations between the preoperative and intraoperative functional data via the use of a multi-modal imaging application platform. The ability to validate these tests with co-registered intraoperative MRI and cortical stimulation testing provides an opportunity to enhance neurosurgeons' ability to define eloquent cortex and avoid neurological injury.

Acknowledgements

The authors gratefully acknowledge support from NIH (K08 NS048063, U41-RR 019703), The Brain Science Foundation, and Brigham and Women's Institute for the Neurosciences. We acknowledge GE Healthcare Navigation (Lawrence, MA) for the development and technical support of Image Fusion and Surgical Navigation products. A.J.G. presently has no financial relationship with GE Healthcare but has served as an unpaid consultant for the development of the navigation System.

References

1. Claus EB, Horlacher A, Hsu L, *et al*. Survival rates in patients with low-grade glioma after intraoperative magnetic resonance image guidance. *Cancer* 2005; **103**: 1227–1233.
2. Hill DL, Maurer CR Jr, Maciunas RJ, *et al*. Measurement of intraoperative brain surface deformation under a craniotomy. *Neurosurgery* 1998; **43**: 514–526.
3. Dorward NL, Alberti O, Velani B, *et al*. Postimaging brain distortion: magnitude, correlates, and impact on neuronavigation. *J Neurosurg* 1998; **88**: 656–662.
4. Ferrant M, Nabavi A, Macq B, *et al*. Serial registration of intraoperative MR images of the brain. *Med Image Anal* 2002; **6**: 337–359.
5. Ojemann JG, Miller JW, Silbergeld DL. Preserved function in brain invaded by tumour. *Neurosurgery* 1996; **39**: 253–258.
6. Black P, Jaaskelainen J, Chabrerie A, *et al*. Minimalist approach: functional mapping. *Clin Neurosurg* 2002; **49**: 90–102.
7. Hirsch J, Ruge MI, Kim KH, *et al*. An integrated functional magnetic resonance imaging procedure for preoperative mapping of cortical areas associated with tactile, motor, language, and visual functions. *Neurosurgery* 2000; **47**: 711–721.
8. Yetkin FZ, Mueller WM, Morris GL, *et al*. Functional MR activation correlated with intraoperative cortical mapping. *Am J Neuroradiol* 1997; **18**: 1311–1315.
9. Roux FE, Boulanouar K, Ibarrola D, *et al*. Functional MRI and intraoperative brain mapping to evaluate brain plasticity in patients with brain tumours and hemiparesis. *J Neurol Neurosurg Psychiat* 2000; **69**: 453–463.
10. Krings T, Schreckenberger M, Rohde V, *et al*. Functional MRI and 18F FDG-positron emission tomography for presurgical planning: comparison with electrical cortical stimulation. *Acta Neurochir (Wien)* 2002; **144**: 889–899.
11. Roux FE, Boulanouar K, Lotterie JA, *et al*. Language functional magnetic resonance imaging in preoperative assessment of language areas: correlation with direct cortical stimulation. *Neurosurgery* 2003; **52**: 1335–1345.
12. Pirotte B, Voordecker P, Neugroschl C, *et al*. Combination of functional magnetic resonance imaging-guided neuronavigation and intraoperative cortical brain mapping improves targeting of motor cortex stimulation in neuropathic pain. *Neurosurgery* 2005; **56**: 344–359.
13. Roux FE, Ibarrola D, Tremoulet M, *et al*. Methodological and technical issues for integrating functional magnetic resonance imaging data in a neuronavigational system. *Neurosurgery* 2001; **49**: 1145–1156.
14. Knierim KE, Petrovich NM, O'Shea JP, *et al*. Pneumatically driven finger movement: a novel, passive fMRI technique for presurgical motor and sensory mapping. Congress of Neurological Surgeons 54th Annual Meeting, 2004.
15. Baddeley A, Emslie H, Nimmo-Smith I. *The Speed and Capacity of Language Processing (SCOLP) Test*. Bury St. Edmunds, Suffolk: Thames Valley Test Company, 1992.
16. Friston K, Holmes A, Worsley K, *et al*. Statistical parametric maps in functional imaging: a general linear approach. *Hum Brain Mapp* 1995; **2**: 189–210.
17. Wells WM III, Viola P, Atsumi H, *et al*. Multi-modal volume registration by maximization of mutual information. *Med Image Anal* 1996; **1**: 35–51.
18. Yoo SS, Talos IF, Golby AJ, *et al*. Evaluating requirements for spatial resolution of fMRI for neurosurgical planning. *Hum Brain Mapp* 2004; **21**: 34–43.
19. Friston KJ, Holmes A, Poline JB, *et al*. Detecting activations in PET and fMRI: levels of inference and power. *Neuroimage* 1996; **4**: 223–235.
20. Maldjian JA, Listerud J, Khalsa S. Integrating postprocessed functional MR images with picture archiving and communication systems. *Am J Neuroradiol* 2002; **23**: 1393–1397.
21. Black PM, Ronner SF. Cortical mapping for defining the limits of tumour resection. *Neurosurgery* 1987; **20**: 914–919.
22. Gering DT, Nabavi A, Kikinis R, *et al*. An integrated visualization system for surgical planning and guidance using image fusion and an open MR. *J Magn Reson Imaging* 2001; **13**: 967–975.
23. McDonald JD, Chong BW, Lewine JD, *et al*. Integration of preoperative and intraoperative functional brain mapping in a frameless stereotactic environment for lesions near eloquent cortex. Technical note. *J Neurosurg* 1999; **90**: 591–598.
24. Krings T, Schreckenberger M, Rohde V, *et al*. Metabolic and electrophysiological validation of functional MRI. *J Neurol Neurosurg Psychiat* 2001; **71**: 762–771.
25. Signorelli F, Guyotat J, Schneider F, *et al*. Technical refinements for validating functional MRI-based neuronavigation data by electrical stimulation during cortical language mapping. *Minim Invasive Neurosurg* 2003; **46**: 265–268.
26. Sobottka SB, Bredow J, Beuthien-Baumann B, *et al*. Comparison of functional brain PET images and intraoperative brain-mapping data using image-guided surgery. *Comput Aided Surg* 2002; **7**: 317–325.
27. Roberts DW, Hartov A, Kennedy FE, *et al*. Intraoperative brain shift and deformation: a quantitative analysis of cortical displacement in 28 cases. *Neurosurgery* 1998; **43**: 749–758.
28. Nimsky C, Ganslandt O, Buchfelder M, Fahlbusch R. Glioma surgery evaluated by intraoperative low-field magnetic resonance imaging. *Acta Neurochir Suppl* 2003; **85**: 55–63.
29. Clatz O, Delingette H, Talos IF, *et al*. Robust nonrigid registration to capture brain shift from intraoperative MRI. *IEEE Trans Med Imaging* 2005; **24**: 1417–1427.
30. Warfield SK, Haker SJ, Talos IF, *et al*. Capturing intraoperative deformations: research experience at Brigham and Women's Hospital. *Med Image Anal* 2005; **9**: 145–162.